Geophys. J. Int. (2004) **159,** 390–399 doi: 10.1111/j.1365-246X.2004.02357.x

Intraplate seismicity in SE Brazil: stress concentration in lithospheric thin spots

Marcelo Assumpção,[1] Martin Schimmel,[1,*] Christian Escalante,[1,†] José Roberto Barbosa,[1] Marcelo Rocha[1] and Lucas V. Barros[2]

[1] *University of São Paulo, IAG, Rua do Matão* 1226, *Cidade Universitária, São Paulo* SP 05508-090, *Brazil. E-mail: marcelo@iag.usp.br*
[2] *Seismological Observatory, University of Brasília, Brasília* 70910, *Brazil*

Accepted 2004 April 29. Received 2004 April 15; in original form 2003 April 16

SUMMARY

Intraplate seismicity has generally poor correlation with surface geological patterns. Except for major extensional features, such as aborted continental rifts, which may act as weak zones, it is usually difficult to find simple geology based models to explain differences in seismic activity in stable continental regions. Seismicity in Brazil is clearly not uniform and a few areas of higher activity have been identified. However, the seismic areas show almost no correlation with the main geological provinces, which is typical of other intraplate settings. A recent upper-mantle tomography study in SE and central Brazil, using approximately 8500 *P*-wave and 2000 *PKP*-wave arrivals recorded in 59 sites since 1992, has mapped *P*-wave velocity anomalies from lithospheric depths down to 1300 km. In this region, higher seismic activity occurs preferentially in areas with low *P*-wave velocities at 150–250 km depth. The low *P*-wave velocities are interpreted as shallower asthenosphere. In such areas, a hotter geotherm will reduce the strength of the lithospheric upper mantle causing most of the intraplate forces to be concentrated in the brittle upper crust. The low-velocity anomalies coincide with Late Cretaceous provinces of alkaline intrusions. The proposed ponding of the Trindade plume head beneath lithospheric thin spots is consistent with our tomography results, suggesting that plume effects may have helped to preserve lithosphere/asthenosphere topography. Although other factors are also important, the present data show that stress concentrations resulting from lithosphere/asthenosphere topography should play an important role in explaining the intraplate seismicity in the Brazilian platform.

Key words: intraplate seismicity, lithospheric strength, Trindade plume, upper-mantle tomography.

1 INTRODUCTION

Understanding the causes of seismicity in stable continental interiors, in most cases, is still a challenge in seismology. Although observations show that seismic activity is not uniform in intraplate areas, it is not always clear why seismicity concentrates in certain regions while others are completely aseismic. One of the major difficulties in studies of intraplate seismicity is that seismic ruptures very rarely reach the surface and in general no correlation is observed between epicentres and old geological faults mapped at the surface (e.g. Seeber & Armbruster 1988; Talwani 1989; Ferreira *et al.* 1998). Several models have been proposed to explain the distribution of seismicity in intraplate areas. In general, the proposed models involve weak zones, stress concentrations from lateral density variation, flexural stresses, or a combination of the above factors.

In a classical review paper, Sykes (1978) attempted to explain intraplate seismicity as resulting from pre-existing zones of weakness. Relatively recent tectonism (such as evidenced by Mesozoic or Cenozoic alkaline intrusions) would indicate deep crustal weakness zones including suture zones, aborted rifts and faults in cratonic limits. For large earthquakes (larger than 6.5 *Ms*) in stable continental regions, Johnston (1989) and Johnston & Kanter (1990) confirmed a good correlation between epicentres and areas affected by extensional Mesozoic tectonism such as passive margins or intracontinental grabens, with the weak zones being the areas of extended continental crust. However, in areas with smaller earthquakes, weak zones are not so easily identified.

Another class of models uses stress concentrations in the crust, which can be caused by lateral density variations, rock rigidity contrast between crustal blocks or flexure from lithospheric loads (see

*Now at: Institute of Earth Sciences, CSIC, Barcelona 08028, Spain.
†Now at: Instituto Geofisico de Arequipa, Peru.

Dewey (1998) for a review). Lateral density variations near mountain chains (e.g. the contrast between the low-density crustal root beneath the chain and the high-density upper mantle in the neighboring shield) causes extensional stresses in the high-topography areas and compressional stresses in the low-lying nearby areas, such as in the Transverse Ranges (Sonder 1990) and in the sub-Andean region (Assumpção & Araujo 1993). The same gravity effect operates in the continental/oceanic transition zone (e.g. Bott & Dean 1972; Stein *et al.* 1989) and was included by Meijer (1995) and Coblentz & Richardson (1996) in their models of mid-plate stresses in South America. High local stresses can also be generated by flexural effects from intracrustal loads, such as proposed by Zoback & Richardson (1996) and Lima *et al.* (1997) for the Middle Amazon basin, or by sedimentary loads in the continental shelf (e.g. Cloetingh *et al.* 1984; Stein *et al.* 1989).

Regional stresses from plate boundary forces can be combined with local effects, resulting from density contrasts or flexure, increasing the resultant stresses (so called superposition model) such as proposed by Lima *et al.* (1997), Assumpção (1998a) and Ferreira *et al.* (1998) to explain the seismicity along parts of the northeastern and southeastern margins of Brazil. However, seismicity along the Brazilian passive margin is not uniform: for example, the superposition model used for the NE margin fails to explain the aseismicity along the northern margin. This means that other factors must be searched for.

It is clear that no simple model can explain all aspects of intraplate seismicity. Detailed understanding of each seismic province may require a combination of many different factors (e.g. Talwani & Rajendram 1991) including different types of crustal weaknesses and various mechanisms of stress concentrations. Also, the concept of weak zones may not be related only to geological features mapped at the surface, but may include all of the rheological profile of the lithosphere. For example, Liu & Zoback (1997) showed an interesting mechanism of stress concentration in the upper crust as a result of a weaker subcrustal lithosphere in the New Madrid seismic zone.

We show that the seismicity in the central and SE Brazilian platform is not uniformly distributed, but no clear correlation with surface geological features can be observed. Upper-mantle tomography studies show *P*-wave, low-velocity anomalies in the 150–250 km depth range, probably related to variations of lithospheric thickness, with a good correlation with concentrations of seismicity. We propose that a thinner lithosphere, with a weaker upper-mantle lid, may concentrate stresses in the brittle upper crust, which may help explain the observed epicentral distribution.

2 SEISMICITY IN SE BRAZILIAN PLATFORM

In this paper, we focus on the continental seismicity of central and SE Brazil. The study area is indicated by the box in Fig. 1 where upper-mantle tomography studies have been carried out recently. Despite the low seismicity level in the SE Brazilian platform (the largest event occurred in 1922 with 5.1 m_b), Fig. 2 shows that the epicentral distribution is not uniform and large aseismic areas can be recognized. The present earthquake catalogue (from the compilation of Berrocal *et al.* 1984, and the Brazilian Seismic Bulletins published

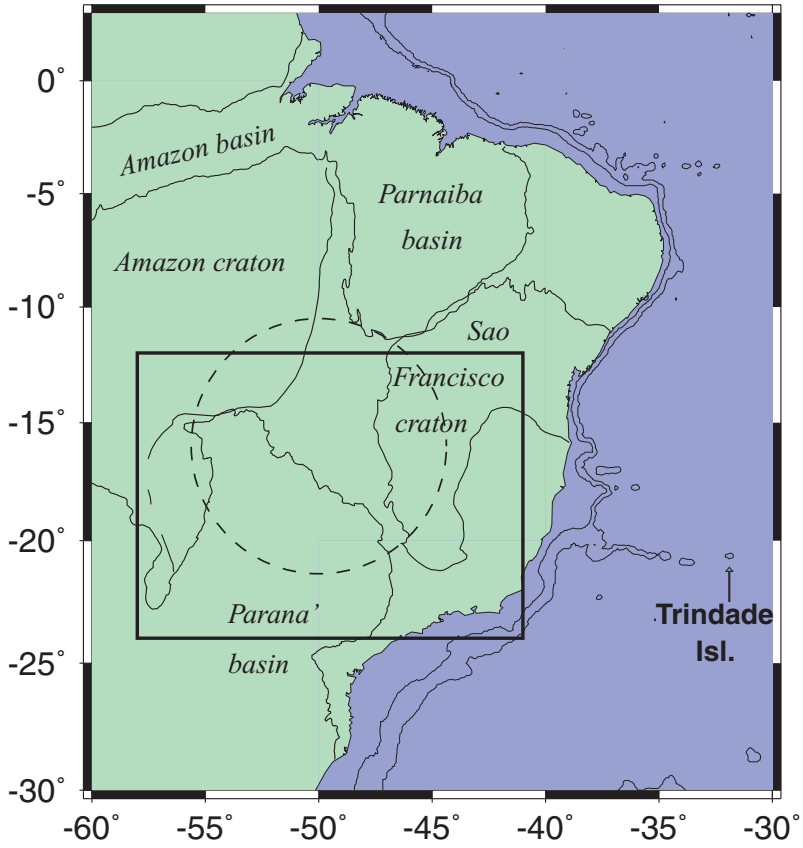

Figure 1. Map of eastern South America showing the study area. The rectangle marks the area shown in Fig. 2. The dashed circle indicates the 600-km radius of the impact zone of the Trindade plume head, at 85–80 Ma, as proposed by Gibson *et al.* (1995, 1997). Contour lines in the ocean are the 200 and 2000-m bathimetry.

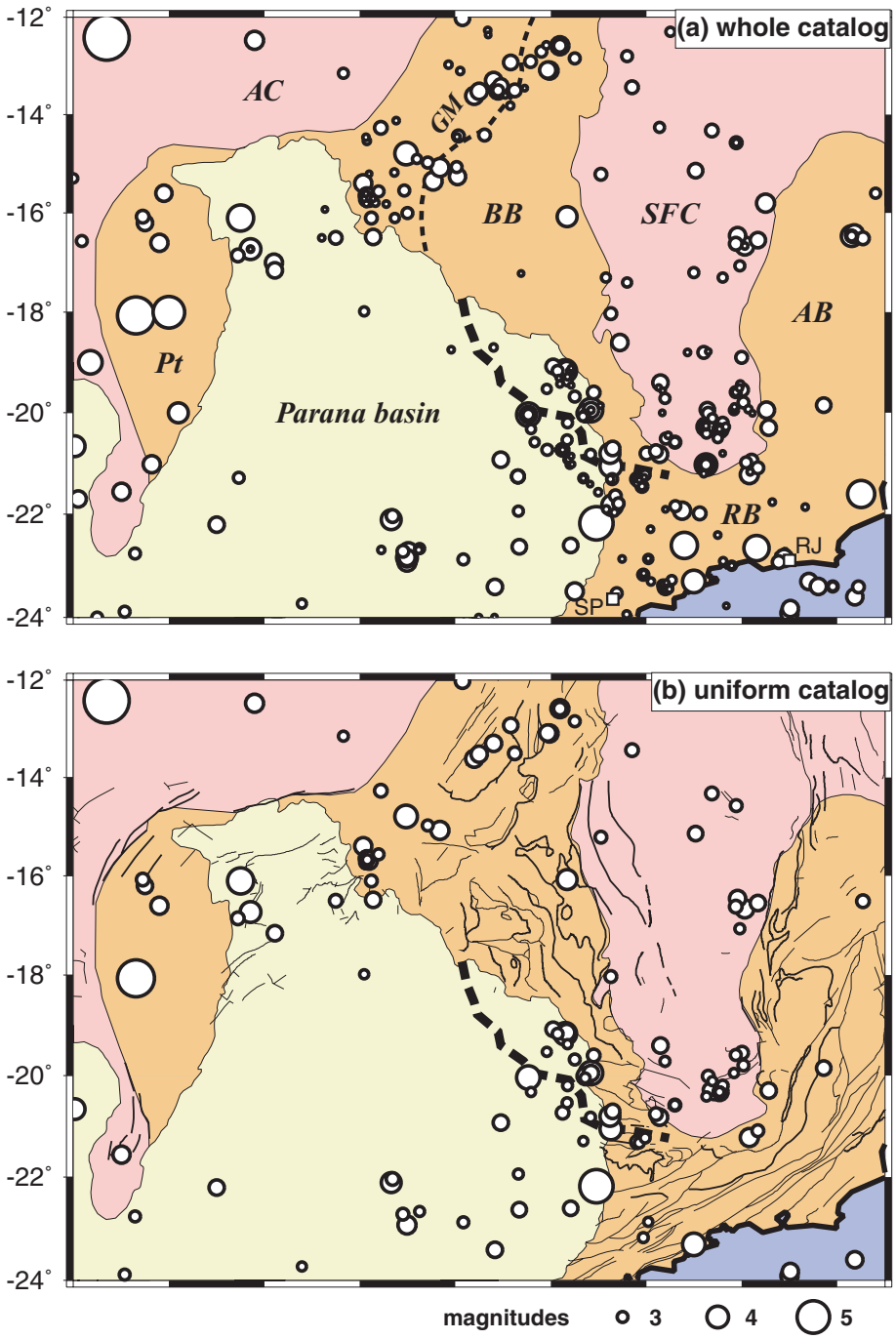

Figure 2. Seismicity maps of SE Brazilian shield. (a) Whole catalogue with all historical and instrumental epicentres. Thin lines denote limits of major geological provinces. Amazon craton (AC), São Francisco craton (SFC), Araçuaí fold belt (AB), Brasília fold belt (BB), Ribeira belt (RB), Pantanal basin (Pt). Thick dashed line is suture zone proposed by Lesquer *et al.* (1981). Thin dashed line is the limit of the Goiás Massif (GM). The Goiás Massif and the Brasília foldbelt are part of the Tocantins province. Squares indicate the cities of São Paulo (SP) and Rio de Janeiro (RJ). (b) Uniform catalogue with events filtered with the time variable thresholds of Table 1. Additional lines denote geological faults from CPRM (2000).

in the Rev. Bras. Geofísica) includes both historical and instrumental data from 1861 to 2003, shown in Fig. 2(a). Its completeness is variable both in time and space. For example, events before 1900 only appear in the region approximately between the cities of São Paulo and Rio de Janeiro (in the Ribeira fold belt), where the population density was higher and accounts of earthquakes felt by the population were recorded in newspapers and books. In the late 1970s and early 1980s many seismographic stations were installed in reservoir areas in the Paraná basin and parts of the surrounding fold belt, allowing events as small as magnitude 2.0 to be located in SE Brazil.

To have a better representation of the geographical distribution of seismicity, this whole catalogue must be filtered to eliminate concentrations of events resulting from a higher population density or a large number of seismographic stations in some particular areas. The threshold magnitude (i.e., the minimum magnitude with a large probability of being detected in the whole southeastern region)

Table 1. Time variation of threshold magnitudes.

Magnitude	Date	Comments
5.0	1900	Macroseismic coverage, 250 km felt radius
4.5	1940	Macroseismic coverage, 100 km felt radius
4.0	1965	Brasilia array and RDJ station
3.2	1980	Regional stations in SE Brazil
2.8	1990	Increase in regional cover

varies with time. Table 1 (adapted from Assumpção 1998a) shows the threshold magnitudes used to produce the uniform catalogue of Fig. 2(b). For example, events larger than magnitude 3.2 are only included in the uniform catalogue if they occurred in 1980 or later, when there were enough seismic stations in SE Brazil to record any event of this size in the area of Fig. 2. A similar threshold (magnitude 3.1) was used for this region by Berrocal *et al.* (1996) for earthquakes after 1979. Since approximately 1990, with the installation of additional digital three-component stations, events down to magnitude 2.8 are believed to be completely detected in the southeastern region (Table 1). Seismicity maps using time-variable threshold magnitudes (e.g. Adams & Basham 1991; Engdahl & Rinehart 1991; Assumpção *et al.* 2002) are useful for recognizing areas with different seismicity rates and better defining seismogenic zones.

The study region (Fig. 2a) has two main Archean/Mesoproterozoic cratonic areas (Amazon and São Francisco cratons) surrounded by Neoproterozoic/Early Palaeozoic fold belts: Brasilia belt between the two cratons, the Ribeira belt along the coast and the Araçuaí belt to the east. The Paraná basin, with Palaeozoic origin, covers parts of the fold belts and may conceal a small cratonic nucleus (Brito Neves & Cordani 1991). The region between the Amazon craton, the São Francisco craton and the Paraná basin is known as the Tocantins province. The Goiás Massif, a narrow block trending roughly SSW–NNE with Archean terranes and the Brasília fold belt are part of the Tocantins province.

The uniform catalogue (Fig. 2b) shows that earthquakes in SE and central Brazil tend to occur more frequently in two main seismic zones: (i) a SW–NE trending zone in the Tocantins province and (ii) the southern part of the Brasília fold belt including a small part of the São Francisco craton and the NE border of the Paraná basin. Fig. 2(b) clearly demonstrates the relative aseismicity of the Ribeira fold belt (Serra da Mantiqueira and Serra do Mar coastal ranges), as compared with the other continental areas. The Paraná basin also seems to be relatively less seismic: the largest events in the basin (magnitudes $\sim$3.5) have been triggered by hydroeletric reservoirs or artesian wells (Berrocal *et al.* 1984; Mioto *et al.* 1991; Yamabe & Berrocal 1991; Assumpção *et al.* 1995; Yamabe & Hamza 1996).

The epicentral distribution (Fig. 2b) shows no obvious correlation with the main geological units described above. Earthquakes occur both in fold belts and in cratonic areas. In fact, the Amazon and São Francisco cratons correspond to 1/3 of the area shown in Fig. 2 and contain also 1/3 of the epicentres of the uniform catalogue. Large sections of the fold belts (such as the central part of Fig. 2, or in the Araçuaí belt, east of the São Francisco craton) are aseismic. A suture zone marking the final collision between the São Francisco craton and a possible cratonic block beneath the Paraná basin (thick dashed line in Fig. 2) has been recognized both by geological studies and by a strong gravimetric gradient (Lesquer *et al.* 1981). This suture zone could be a candidate for a weak zone but Fig. 2 shows that seismicity only occurs near its SE segment, with the northern segment being completely aseismic. A correlation has been suggested between the SW–NE trending seismic belt in the Tocantins province and the regional structural trend (Fig. 2). However, a closer examination shows that the seismic belt crosses several different geological blocks, such as the Goiás Massif and the foreland domain of the Brasília belt (Fig. 2a).

3 UPPER-MANTLE TOMOGRAPHY

Upper-mantle, *P*- and *S*-wave traveltime tomography has been carried out in SE Brazil since 1992 (VanDecar *et al.* 1995; Schimmel *et al.* 2003) using mainly temporary broad-band stations. A few permanent stations of the global network as well as short-period regional stations have also been used. Until 2003, 59 sites in SE and central Brazil (Fig. 3a) produced a total of 8500 *P*-wave and 2000 *PKP*-wave readings (Escalante 2002; Rocha 2003). Relative traveltime residuals were obtained by cross-correlation techniques using *P*-wave phases from teleseismic distances and also *PKP*-df phases. In addition to *P*-wave anomalies, the inversion included station corrections and small (heavily damped) epicentral mislocation. Smoothness constraints (minimizing both 1st and 2nd model derivatives) were used to regularize the inversion. Residuals larger than 1.5 standard deviations were downweighted to reduce effects of possible outliers. The model area is approximately that shown in Fig. 3(a), with velocity anomalies defined in a grid with node spacing approximately 33 km in the NS and EW directions and 33 km in depth, in the better resolved area of the model. The inverted model, extends down to 1300-km depth. More details of the inversion technique are described in VanDecar *et al.* (1995) and Schimmel *et al.* (2003). The input data consisted of relative residuals ranging roughly from -1 to $+1$ s (rms of 0.41 s). After the inversion, the tomographic model explained approximately 88 per cent of the data, with final residuals having rms deviations of approximately 0.05 s.

Fig. 3 shows the *P*-wave velocity variations at depths of 150 and 200 km. Dark areas denote poorly resolved parts of the model with insufficient ray samplings. Because only relative arrival times were picked (and not absolute traveltimes), only lateral velocity anomalies are obtained in the tomography inversion, i.e. variations of *P*-wave velocity relative to a 1-D model. This means that the high- and low-velocity anomalies shown in Fig. 3 refer to the average velocity at each depth.

The São Francisco craton, as expected, is characterized by larger than average *P*-wave velocities. The middle part of the Paraná basin has mainly high velocities, consistent with the hypothesis of a cratonic block beneath the basin. However, the largest positive anomaly can be seen in the Brasília belt, near the NE border of the Paraná basin, a feature not yet completely understood. A strong negative anomaly is seen in the Tocantins province (approximately 16°S, 51°W) coincident with the Iporá igneous province (a set of 85–60 Ma alkaline intrusions, shown in Fig. 3a). As pointed out by Schimmel *et al.* (2003), low velocities are also observed near the Alto Paranaíba Igneous province (APIP) of the same age, as well as further to the east, near the coast, where the alkaline intrusions are slightly younger (85–50 Ma). Another igneous province (Poxoréu, near the northwestern edge of the Paraná basin) also seems to be characterized by low velocities. These igneous provinces may be related to a proposed Trindade plume (Gibson *et al.* 1995, 1997) whose latest track would be the E–W trending Vitoria–Trindade island chain in the Atlantic as seen in Fig. 1. The initial impact of the plume would have occurred beneath the Iporá province; the spread of the plume head, as indicated by the dashed circle in Fig. 1, caused the other igneous provinces by ponding plume material beneath areas of thinner lithosphere, according to Gibson *et al.* (1997).

It is interesting to note that the older, 140–120 Ma intrusions (red circles in Fig. 3a) do not correlate with low velocities in the

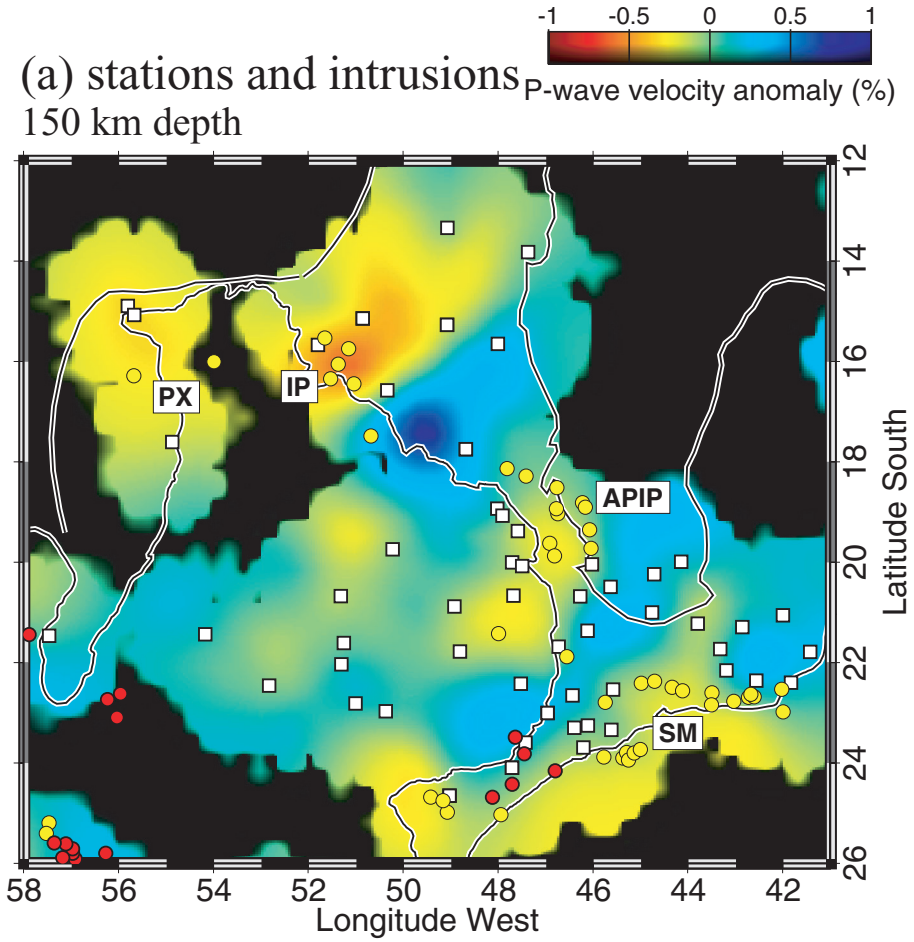

Figure 3. *P*-wave anomalies in SE Brazil. (a) Anomalies at 150-km depth. Squares denote seismic stations used in the tomography. Circles indicate alkaline intrusions: red circles denote Upper Jurassic/Lower Cretaceous intrusions (140–120 Ma) roughly contemporaneous with the South Atlantic rifting and the extrusion of flood basalts in the Paraná basin; yellow circles are Upper Cretaceous/Early Terciary (85–50 Ma) intrusions; note that the more recent intrusions tend to occur at or near the borders of *P*-wave, low-velocity anomalies. Poxoréu igneous province (PX), Iporá alkaline province (IP); Alto Paranaíba Igneous province (APIP); Serra do Mar province (SM). (b) Anomalies at 200-km depth with epicentres (circles) from the uniform catalogue of Fig. 2(b); note concentration of events near areas of lower *P*-wave velocities.

bottom of the lithosphere. These older intrusions were probably related to the impact of the Tristan da Cunha superplume during the South Atlantic rifting. Fig. 4 shows the distribution of the *P*-wave anomalies beneath the older and beneath the more recent Late Cretaceous/Palaeogene magmatism. The velocity anomaly beneath each alkaline outcrop was taken as the average in a window of $\pm 1^\circ$ between 100- and 300-km depth. The mean velocity anomaly beneath the whole study area of Fig. 3 is +0.03 per cent. The mean velocity anomaly beneath the 85–50 Ma intrusions is significantly lower than this regional average; the anomalies beneath the older intrusions are higher than the regional average. This supports the hypothesis that the low velocities beneath the alkaline provinces are the residual thermal effects of mantle upwellings impacting areas of thinner lithosphere, which would be consistent with a possible Trindade plume head.

4 SEISMICITY AND LOW-VELOCITY ANOMALIES

Fig. 3(b) shows a clear trend of the seismicity to be located in areas with low velocities in the uppermost mantle. The epicentres shown in Fig. 3(b) are those of the uniform catalogue of Fig. 2(b). The SW–NE trending seismic belt in the NW part of the Tocantins province is located in a region with negative velocity anomalies in the uppermost mantle. This seismic belt seems to continue beneath the Poxoréu igneous province (PX) and the Pantanal basin following the low-velocity anomalies. The concentration of epicentres next to the southern part of the São Francisco craton, along the southern segment of the suture zone (Fig. 2b), also occurs in a region with lower than average velocities in the upper mantle. The area of highest velocites near the NE border of the Paraná basin, on the other hand, is completely aseismic. Some exceptions are observed in the São Francico craton and the middle of the Paraná basin, but these events are generally small with magnitude less than 3.7 m_b.

To quantify the visual correlation seen in Fig. 3(b), we compared the distribution of the *P*-wave velocity anomalies in the subcrustal lithosphere in the seismic and aseismic areas. A grid with 0.5° spacing was used to sample the study region (central and SE Brazil as shown in Fig. 3b). For every point in this grid, we calculated the energy of all earthquakes within a 40-km radius. The magnitude corresponding to this total energy was called cumulative magnitude. For every point in the grid, we also calculated the average velocity anomaly within a window of $\pm 0.5^\circ$ and depth interval 150–250 km. Fig. 5 shows the distribution of the velocity anomalies in the

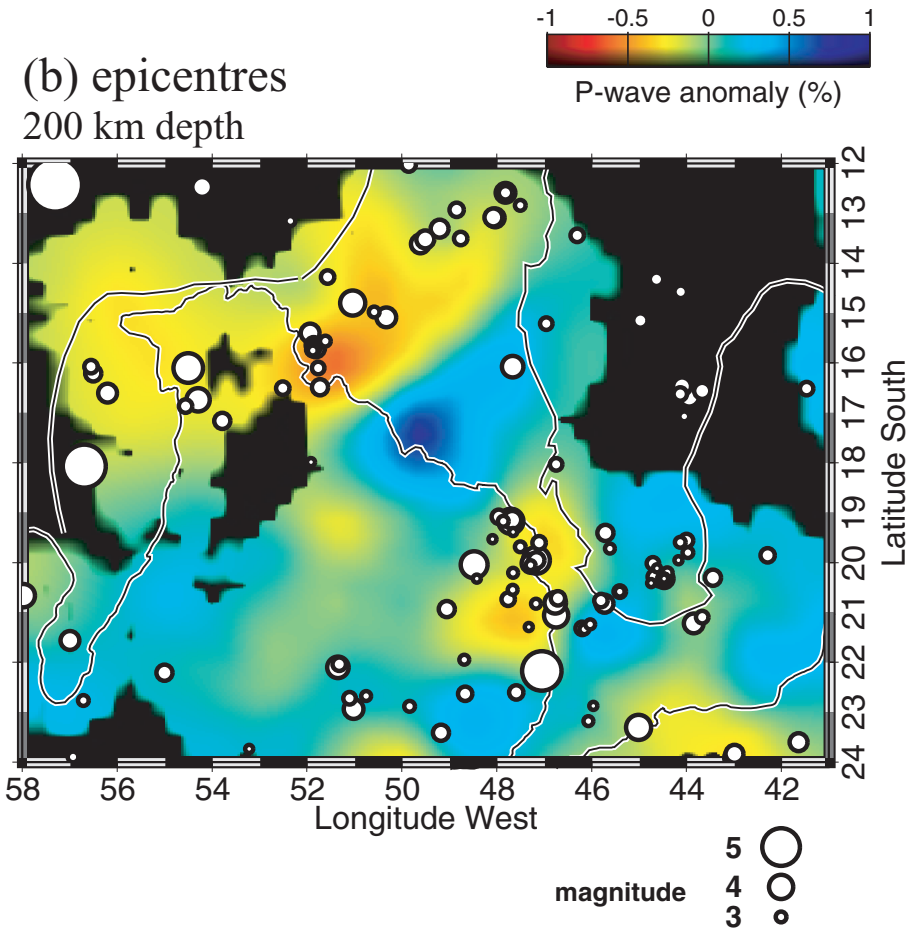

Figure 3. (*Continued.*)

gridpoints with high seismicity (cumulative magnitude $\geq$4), low seismicity (m_b < 4), and aseismic points (no events). Only gridpoints with enough ray density in the tomography inversion were used: i.e., darkened areas in Fig. 3 were not included in Fig. 5. The mean *P*-velocity anomaly in all the study area, at 200-km depth, is 0.03 per cent. The mean velocity in areas with high activity (magnitude $\geq$4) is lower than this regional average (Fig. 5, top), whereas aseismic areas have a mean *P* velocity slightly higher than the regional average (Fig. 5, bottom). Areas with intermediate activity (m_b < 4) show a slight trend towards lower velocities, but are not significantly different from the aseismic areas (Fig. 5, middle). The standard deviations of these means are approximately 0.03, indicating that the difference between the mean velocities beneath the seismic and aseismic areas is highly significant. We also tested taking the average anomaly and cumulative magnitude every 1°, within a larger radius, and the histograms showed similar patterns. When seismicity is compared with the *S*-wave anomalies mapped by Schimmel *et al.* (2003), the same trend is suggested. This is not surprising as *P*-wave and *S*-wave anomalies are usually well correlated.

5 DISCUSSION

Seismic velocity anomalies in the upper mantle can be caused both by temperature and composition variations, especially if the anomalies are small such as shown in Fig. 3. However, we believe that lateral temperature variation is a major factor contributing to the observed velocity anomalies. Several lines of evidence support this hypothesis. First, Schimmel *et al.* (2003) showed that upper-mantle *P*- and *S*-wave anomalies in SE Brazil have a similar pattern, such as high velocities beneath the São Francisco craton and beneath the middle of the Paraná basin, and low velocities near the APIP (*S*-wave data for the Tocantins province have not been fully analysed yet). This is consistent with temperature anomalies, which affect both *P* and *S* velocities in the same direction. Secondly, the fact that only the more recent (85–50 Ma) alkaline intrusions occur near low-velocity areas may indicate a thermal effect associated with the generation of the Late Cretaceous igneous activity. Thirdly, heat flow data in SE Brazil (Hamza & Muñoz 1996; Hurter & Pollack 1996) show a trend of lower heat flow density in the middle of the Paraná basin (approximately 40 to 50 mW m^{-2}) compared with the border of the basin and surrounding fold belts (approximately 50 to 60 mW m^{-2}). This is consistent with the generally higher *P*-wave velocities in the middle of the basin and the fact that the low-velocity anomalies are observed near the borders of the basin.

The velocity anomalies obtained from the tomographic inversion are lower bounds because of smoothness constraints necessary to regularize the tomographic inversion. In addition, station corrections are also inverted for and can absorb part of the signal produced by velocity anomalies at lithospheric depths. Synthetic tests (Schimmel *et al.* 2003) show that we usually recover approximately 50 to 70 per cent of the actual anomalies. The mean anomalies in the seismic and aseismic areas (Fig. 3b) differ by approximately 0.5 per

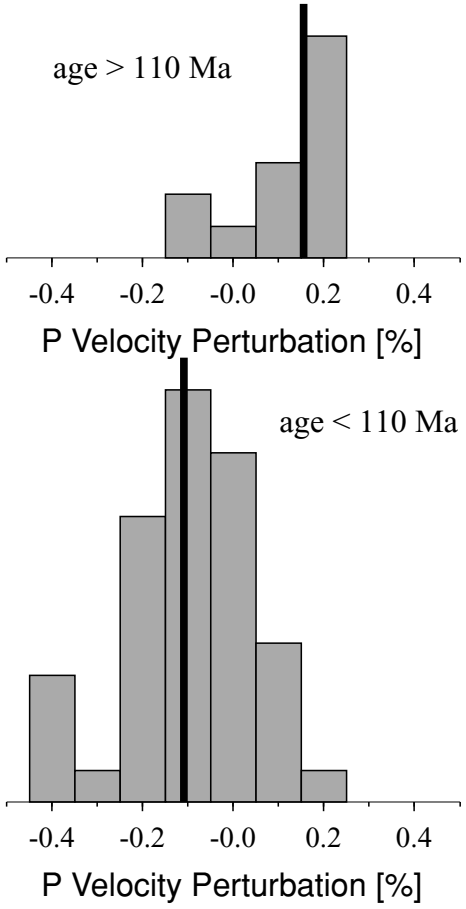

Figure 4. Distribution of *P*-wave velocity anomalies in the subcrustal lithosphere beneath outcrops of alkaline intrusions. Top: 140–120 Ma. Bottom: 85–50 Ma. The vertical lines denote the medium values of each distribution. Younger intrusions tend to occur in areas with lower than average anomalies, possibly indicating a thermal origin for the lower velocities.

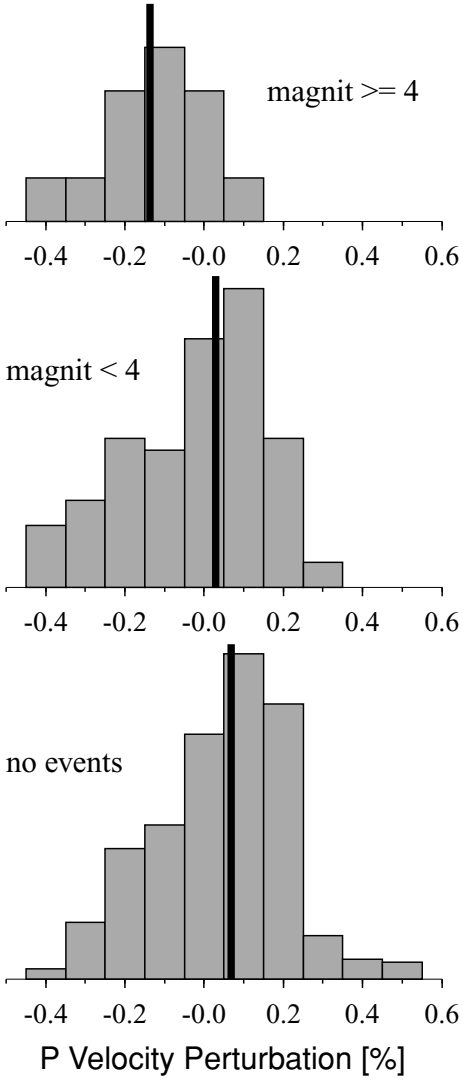

Figure 5. Distribution of *P*-wave velocity anomalies in the subcrustal lithosphere according to seismicity level. Average anomalies were computed in boxes of ±0.5 ° from 150–250 km depth. Top: histogram of *P*-wave anomalies beneath areas with cumulative magnitudes ≥4. Middle: anomalies beneath areas with cumulative magnitudes <4. Bottom: anomalies beneath areas with no earthquakes. The vertical lines denote the medium values of each distribution. Note the trend of seismicity to occur in areas with lower than average *P*-wave anomaly.

cent implying a real difference of the order of 0.7 to 1.0 per cent. A *P*-wave velocity anomaly of 0.5–1.0 per cent may correspond to a temperature variation of approximately 70–150 °C, using the average upper-mantle mineral coefficients compiled by Anderson & Isacks (1995) and Qiu *et al.* (1996). More accurate estimates of upper-mantle temperature variations from velocity anomalies require knowledge of the absolute seismic velocity and temperature because of the non-linear nature of the velocity/temperature derivatives (Cammarano *et al.* 2003). If we use the AK135 velocity model (Kennett *et al.* 1995) more representative of continental areas and a reference geotherm corresponding to the 1000 °C adiabat, consistent with the AK135 velocities (Cammarano *et al.* 2003), a 1 per cent velocity anomaly will imply a temperature contrast of 150 °C at 100-km depth or 200 °C at 200 km. These differences are quite compatible with the geotherms used to calculate the strength envelopes in Fig. 6 below. This temperature contrast makes the thermal lithosphere thinner in the low-velocity (more seismically active) areas.

We explain the seismicity as resulting from stress concentrations in the upper crust because of weakness in the lithospheric upper mantle. Enough weakness can be caused by temperature anomalies of the order of 100 °C. Fig. 6 shows representative geotherms for the hot/thin lithosphere (low-velocity areas) and the cold/thick lithosphere (high-velocity areas) using a two-layer model for the crust (granitic upper crust and intermediate-to-mafic, granulite lower crust, each 20-km thick) with an ultrabasic upper mantle. Thermal conductivities and heat production constants were taken from Liu & Zoback (1997). The geotherm for the cold area was obtained for a surface heat flow of 50 mW m^{-2}. The temperatures in the upper mantle are higher than those estimated by Liu & Zoback (1997) for the cratonic central and eastern part of the USA, but are lower than the estimates of Artemieva & Mooney (2001) for the area of the Paraná basin. The hot geotherm was calculated for a 55 mW m^{-2} heat flow density at the border of the Paraná basin (Hurter & Pollack 1996) and is approximately 100 °C higher than the cold geotherm in the topmost lithospheric upper mantle. It is not as hot as the geotherm used by Liu & Zoback (1997) for the New Madrid rift zone, where the heat flow is 60 mW m^{-2}. For the yield stress envelopes we used Byerlee's law for a wet granite for the brittle

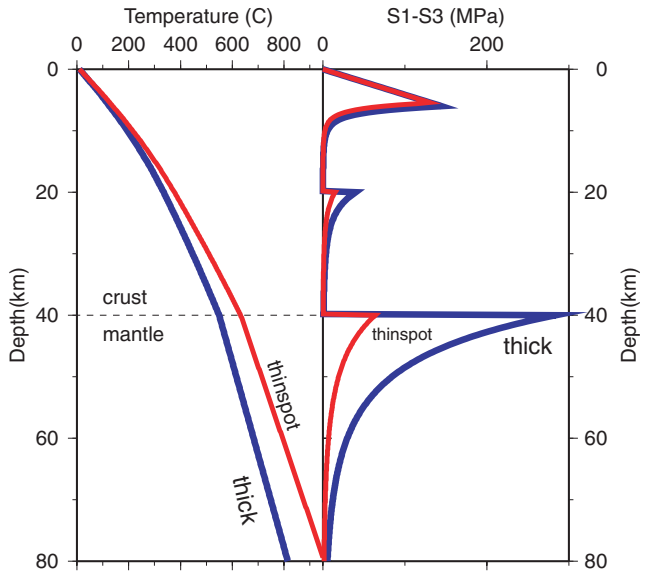

Figure 6. Temperature and yield stress profiles for thick lithosphere (cool/stable areas with heat flow density of 50 mW m^{-2}) and thin lithosphere (hot/active provinces with heat flow density of 55 mW m^{-2}). The same thermal and rheological properties are used for both cases.

limits; for the ductile rheology we used the Adirondack, weak, felsic, granulite model for the lower crust (Wilks & Carter 1990) and the average strength, Anheim, dunite model for the upper mantle (Carter & Tsenn 1987). We used a strain rate of 10^{-18} s^{-1} as usually assumed for stable continental areas such as North America (e.g. Liu & Zoback 1997). Differences in crustal properties can be important in the overall lithospheric strength. However, we used the same crustal structure for both regions because our main interest here is to study the effect of temperature differences in the upper mantle.

Fig. 6 shows that an increase of only 100 °C in upper-mantle temperature can be sufficient to cause considerable weakness in the lithospheric lid. The total strength of the lithosphere, i.e. the total deviatoric force the lithosphere can support for the assumed strain rate of 10^{-18} s^{-1}, can be calculated from the area under the S1–S3 curves in Fig. 6. This integrated strength of the lithosphere can decrease from 3.2×10^{12} to 1.1×10^{12} N m^{-1}. The strength of the upper-mantle part of the lithosphere for the cold and the warm areas would be 2.5×10^{12} and 0.6×10^{12} N m^{-1}, respectively. As in most intraplate areas, the average stress magnitude in the Brazilian lithosphere is not known and we have to rely on theoretical estimates. Numerical models of plate driving forces, using finite-element calculations (Meijer 1995; Coblentz & Richardson 1996), predict strike-slip stress regime in SE and central Brazil with EW compressional axis (S1) and NS tensional axis (S3). The predicted direction and type of stresses are quite consistent with the observed data (Assumpção 1998b). Both numerical models use an elastic 100-km-thick lithosphere and predict stress differences (S1–S3) ranging from 10 to 14 MPa. An average stress of 12 MPa would imply a total lithospheric force of 1.2×10^{12} N m^{-1}. The 100-km-thick elastic layer used in the models of plate driving forces (Meijer 1995; Coblentz & Richardson 1996) is clearly an oversimplification and the calculated average stress (10–14 MPa in our case) is only an equivalent way of expressing the total lithospheric force. This means the estimated total force of 1.2×10^{12} N m^{-1} is a more robust result than the average stress of 12 MPa. Using this estimated total force, we can conclude that a hot lithospheric mantle (with strength of only 0.6×10^{12} N m^{-1}) would not be strong enough and would lead to stress concentration in the brittle upper crust. A cold lithospheric mantle, on the other hand, with a strength of 2.5×10^{12} N m^{-1}, would be able to support all of the intraplate force, leaving the upper crust below the critical stress limit for brittle failure.

Rheological properties of the lower crust and upper mantle are subject to very high uncertainties and stress envelopes, such as shown in Fig. 6, are clearly an oversimplification. We used power-law relations for the crust and upper mantle representative of deformation mechanism dominated by dislocation creep. The temperature and strain rate we used indicate that power law is probably the best description for the deformation mechanism in the topmost upper mantle (Carter & Tsenn 1987). If other creep mechanisms dominate at lower temperatures in the crust, the crustal contribution to the total lithospheric strength would be even lower. However, this would not change our main conclusions that an increase in upper-mantle temperatures of 100–150 °C considerably reduces lithospheric strength. For example, Tommasi & Vauchez (1997), using a higher strain rate, showed that an increase of approximately 75 °C in the lithospheric lid (resulting from a heat flow increase from 60 to 65 mW m^{-2}) reduces to half the total lithospheric strength.

We suggest that the higher temperatures beneath the seismic areas and the alkaline provinces are a remnant effect of hot mantle upwellings trapped in lithospheric thin spots, such as beneath the Iporá and the APIP. This is consistent with the Trindade plume model of Gibson *et al.* (1997) and Thompson *et al.* (1998). Beneath these thin spots, temperature and pressure conditions allowed partial melting of lower lithospheric material to generate the alkaline igneous intrusions (Gibson *et al.* 1995, 1997). Lithospheric thickness at the time of the plume impact seems to have been quite variable in central and SE Brazil. Thermobarometric data from the PX (Fig. 3a) indicate a lithospheric thickness less than approximately 80–100 km (Gibson *et al.* 1997), whereas beneath the APIP the lithosphere would be at least 150-km thick (Gibson *et al.* 1995). Intermediate thickness is suggested by Gibson *et al.* (1997) for the Iporá province. Considering that our limited data near Poxoréu (Fig. 3a) probably causes more smearing of the anomalies, our results (stronger velocity anomalies beneath the PX and the Iporá alkaline province (IP) than beneath the APIP) are generally consistent with the geochemical model. If we take into account that the southern part of the São Francisco craton has a 200–250 km root at present, according to the tomography results (Schimmel *et al.* 2003), then the catchment areas for ponding plume material approximately 80 Ma could have ranged from 50 up to 150 km in height. A 100-km difference in lithospheric thicknesses between cratonic areas and adjacent fold belts is often used in numerical modelling (e.g. Sleep 2003).

Temperature in the bottom of a cold lithosphere can be approximately 1100 °C at 200-km depth. A hot plume material (∼1500 °C) beneath a thin lithosphere gives rise to approximately 400 °C lateral excess temperature in the catchment volume. This temperature difference will decrease both by conduction and convection. If we assume a trapped volume approximately 200 km wide (the rough size of the low-velocity anomaly areas, Fig. 3) and 100 km thick, the maximum temperature of the trapped material will decrease by conduction to approximately half of its initial temperature and the present temperature anomaly would be approximately 200 °C. Convection of the plume material, however, speeds up cooling. Numerical modelling by Sleep (2003) shows that after 40 Myr almost no plume material is left in the catchment volume. Even so, the ponded plume material will help keep the initial temperature

difference between a thick craton (say, 1100 °C at 200-km depth) and the normal asthenospheric adiabat (1300 °C).

Temperature profiles in the deep continental lithosphere cannot be determined accurately, specially in SE Brazil where little is known of upper-mantle properties. Estimates of rheological parameters and convection patterns are even more uncertain. However, it is not the scope of this paper to determine all upper-mantle properties, but only to show that the observed *P*-wave, low-velocity anomalies and the preferential location of Late Cretaceous intrusions are consistent with the hypothesis of a weaker lithosphere caused by higher temperature beneath the seismically active areas.

The correlation of the continental Late Cretaceous/Palaeogene magmatism and the Vitória–Trindade island chain to a common hotspot/plume mechanism is highly controversial. Geochemical similarities between the various igneous provinces, from the Poxoréu province to the Trindade island (Fodor & Hanan 2000; Greenwood 2001), are consistent with a common hotspot origin (Gibson *et al.* 1995, 1997; Thompson *et al.* 1998). Combination of intraplate stress field changes and the Trindade hotspot source has been used by Cobbold *et al.* (2001) to explain the late Cretaceous/Palaeogene reactivation of the pre-existing structures in the continental margin of SE Brazil. However, Riccomini *et al.* (2004) note that the magmatism was not restricted to a single hotspot trace, but was widespread from southern Brazil (Late Cretaceous, Piratini province) to Paraguay (Palaeogene, Asuncion province), approximately 1200 and 1500 km, respectively, from the assumed Trindade hotspot trace. In addition, recent determinations of Ar–Ar ages at several igneous intrusions in the Serra do Mar province seem inconsistent with a pattern of eastward decreasing ages expected from a hotspot source. For these reasons, instead of the plume/hotspot model, Riccomini *et al.* (2004) favour several different pulses of mantle upwellings and stress field changes for the generation and emplacement of alkaline magmas along reactivated regional structures. The correlation we presented between seismicity, low seismic velocities and young igneous intrusions confirm a thermal mechanisms for the Late Cretaceous/Palaeogene activity and we hope will contribute to the Trindade hotspot debate.

6 CONCLUSIONS

Three indirect evidences suggest that the *P*-wave, low-velocity anomalies are mainly caused by higher temperatures: (i) similarity of the *P*- and *S*-wave anomaly patterns, (ii) generally higher heat flow at the border of the Paraná basin where most of the low-velocity anomalies are found and (iii) correlation with the younger post-rift igneous provinces. The lithosphere/asthenosphere topography found by our *P*-wave tomography is in excellent agreement with the thin spot hypothesis proposed by Gibson *et al.* (1995, 1997) for the origin of the igneous provinces. The temperature induced thinning of the lithosphere also correlates with the areas of higher seismicity, indicating an important mechanism to help explain earthquake activity in SE and central Brazil. Thinning of the lithosphere decreases the overall lithospheric strength and causes the regional stress field to concentrate at the brittle upper crust.

Many other different mechanisms have been proposed to explain intraplate seismicity patterns involving weak crustal zones (identified from geological/geophysical studies) and concentration of stresses as a result of lateral structure variation. Usually several mechanisms must be combined to explain all seismicity features in a given region. Here, we showed that deep lithospheric structure can also make an important contribution to help explain the seismicity distribution in the Brazilian platform.

Similar examples have been found in other areas. In the seismically active New Madrid rift, where the surface heat flow averages 60 mW m^{-2}, Liu & Zoback (1997) showed that the higher geotherm causes considerable weakness in the subcrustal lithosphere, compared with the more stable shield region, irrespective of which rheological model is used for the crustal and upper-mantle rocks. Another example has been given by Yang & Liu (2002) in modelling intraplate stresses in China. The higher seismicity of the north China block, compared with the more stable south China block, is better explained with a thin and weak lithosphere as evidenced by *P*-wave, low-velocity anomalies in the upper mantle. New Madrid and China are two of the most seismically active intraplate regions in the world. Our results for Brazil indicate that temperature induced lithospheric weakness can also be an important factor even in areas with very low seismicity levels.

ACKNOWLEDGMENTS

Work supported by Brazilian grants FAPESP 96/01556-0, 97/03640-6, 01/06066-6, 01/01867-0, 02/09989-0 and CNPq 30.0227/79-5, 52.0078/00-4. The authors thank Yára Marangoni for calculating the geotherms and for critically reading the manuscript, and Luís Galhardo for equipment service and maintenance during the tomography experiment. The authors also thank Alain Vauchez, Cláudio Riccomini and Garry Karner for helpful discussions. Suzan Van der Lee and an anonymous reviewer made valuable comments to improve the manuscript.

REFERENCES

Adams, J. & Basham, P.W., 1991. The seismicity and seismotectonics of eastern Canada, in *Neotectonics of North America*, Decade Map Vol. 1, 261–276, eds Slemmons, D.B. et al, Geol. Soc. Am., Boulder, CO, USA.

Anderson, O.L. & Isacks, D.G., 1995. Elastic constants of mantle minerals at high temperature, in, *Mineral Physics and Crystalography: a handbook of physical constants*, Vol. 2, pp. 64–97, ed. Ahrens, T.J., AGU, Washington, DC.

Artemieva, I.M. & Mooney, W.D., 2001. Thermal thickness and evolution of Precambrian lithosphere: a global study, *J. geophys. Res.,* **106**(B8), 16 387–16 414.

Assumpção, M., 1998a. Seismicity and stresses in the Brazilian passive margin, *Bull. seism. Soc. Am.,* **88**(1), 160–169.

Assumpção, M., 1998b. Focal mechanisms of small earthquakes in SE Brazilian shield: a test of stress models of the South American plate, *Geophys. J. Int.,* **133,** 490–498.

Assumpção, M. & Araujo, M., 1993. Effect of the Altiplano-Puna plateau, South America, on the regional intraplate stress, *Tectonophysics,* **221,** 475–496.

Assumpção, M., Freire, M. & Ribotta, L.C., 1995. Sismicidade induzida no reservatório de Capivara: resultados preliminares sobre localização de fraturas ativas. In: *IV Int. Congr. Brazilian Geophys. Soc., Rio de Janeiro, 1995, Proceedings,* **2,** 961–964.

Assumpção, M. *et al.,* 2002. Reservoir induced seismicity in Brazil, *Pure appl. Geophys.,* **159,** 597–617.

Berrocal, J., Assumpção, M., Antezana, R., Dias Neto, C.M., Ortega, R., França, H. & Veloso, J., 1984. *Sismicidade do Brasil*, Instituto Astronômico e Geofísico, Universidade de São Paulo, São Paulo, Brazil, p. 320.

Berrocal, J., Fernandes, C., Bassini, A. & Barbosa, J.R., 1996. Earthquake hazard assessment in southeastern Brazil, *Geofísica Internacional,* **35,** 257–272.

Bott, M.H.P. & Dean, D.S., 1972. Stress systems at young continental margins, *Nature Phys. Sci.,* **235,** 23–25.

Brito Neves, B. & Cordani, U., 1991. Tectonic evolution of South America during the Late Proterozoic, *Precambrian Res.,* **53,** 23–40.

Cammarano, F., Goes, S., Vacher, P. & Giardini, D., 2003. Inferring upper-mantle temperatures from seismic velocities, *Phys. Earth planet. Int.,* **138,** 197–222.

Carter, N.L. & Tsenn, M.C., 1987. Flow properties of continental lithosphere, *Tectonophysics,* **136,** 27–63.

Cloetingh, S.A.P.L., Wortel, M.J.R. & Vlaar, N.J., 1984. Passive margin evolution, initiation of subduction and the Wilson cycle, *Tectonophysics,* **109,** 147–163.

Coblentz, D.D. & Richardson, R.M., 1996. Analysis of the South American intraplate stress field, *J. geophys. Res.,* **100,** 20 245–20 255.

Greenwood, J.C., 2001. The secular geochemical evolution of the Trindade mantle plume, *PhD thesis,* Cambridge Univ., Cambridge, UK.

Cobbold, P.R., Meisling, K.E. & Mount, V.S., 2001. Reactivation of an obliquely rifted margin, Campos and Santos basins, southeastern Brazil, *Am. Assoc. Petrol. Geol. Bull.,* **85**(11), 1925–1944.

CPRM, 2000. *Geologic Map of South America*, 1:5000 000, Brazilian Geological Survey, Brasilia, Brazil.

Dewey, J.W., 1988. Midplate seismicity exterior to former rift-basins. Seismol. Res. Lett., **59,** 213–218.

Engdahl, E.R. & Rinehart, W.A., 1991. Seismicity map of North America Project, in *Neotectonics of North America*, Decade Map Vol. 1, pp. 21–27, eds Slemmons, D.B. *et al.,* Geological Soc. Am., Boulder, CO, USA.

Escalante, C., 2002. Upper mantle *P*-wave tomography beneath SE Brazil, *MPhil thesis*, IAG, University of São Paulo, São Paulo, Brazil (in Portuguese).

Ferreira, J., Oliveira, R.T., Takeya, M.K. & Assumpção, M., 1998. Superposition of local and regional stresses in NE Brazil: evidence from focal mechanisms around the Potiguar marginal basin, *Geophys. J. Int.,* **134,** 341–355.

Fodor, R.V. & Hanan, B.B., 2000. Geochemical evidence for the Trindade hotspot trace: Columbia seamount ankaramite, *Lithos,* **51,** 293–304.

Gibson, S.A., Thompson, R.N., Leonardos, O.H., Dickin, A.P. & Mitchell, J.G., 1995. The late Cretaceous impact of the Trindade mantle plume: evidence from large-volume, mafic potassic magmatism in SE Brazil, *J. Petrol.,* **36**(1), 189–228.

Gibson, S.A., Thompson, R.N., Weska, R.K., Dickin, A.P. & Leonardos, O.H., 1997. Late Cretaceous rift-related upwelling and melting of the Trindade starting mantle plume head beneath western Brazil, *Contrib. Mineral Petrol.,* **126,** 303–314.

Hamza, V.M. & Muñoz, M., 1996. Heat flow map of South America, *Geotherm,* **25**(6), 599–646.

Hurter, S.J. & Pollack, H.N., 1996. Terrestrial heat flow in the Paraná Basin, southern Brazil, *J. geophys. Res.,* **101**(B4), 8659–8671.

Johnston, A.C., 1989. The seismicity of stable continental interiors, in, *Earthquakes at North-Atlantic Passive Margins: Neotectonics and Postglacial Rebound*, pp. 299–327, eds Gregersen, S. & Basham, P.W., Kluwer Academic, Boston, USA.

Johnston, A.C. & Kanter, L.R., 1990. Earthquakes in stable continental crust, *Scientific American,* **262,** 68–75.

Kennett, B.L.N., Engdahl, E.R. & Bulland, R.P., 1995. Constraints on seismic velocities in the Earth from travel times, *Geophys. J. Int.,* **122,** 108–124.

Lesquer, A., Almeida, F.F.M., Davino, A., Lachaud, J.C. & Maillard, V., 1981. Signification structurales des anomalies gravimetriques de la partie sud du craton de S. Francisco (Brésil), *Tectonophysics,* **76,** 273–293.

Lima, C., Nascimento, E. & Assumpção, M., 1997. Stress orientations in Brazilian sedimentary basins from breakout analysis—implications for force models in the South American plate, *Geophys. J. Int.,* **130**(1), 112–124.

Liu, L. & Zoback, M.D., 1997. Lithospheric strength and intraplate seismicity in the New Madrid seismic zone, *Tectonics,* **16**(4), 585–595.

Meijer, P.T., 1995. Dynamics of active continental margins: the Andes and the Aegean region, *PhD thesis,* Utrecht University, the Netherlands, p. 218.

Mioto, J.A., Ribotta, L.C. & Verdiani, A.C., 1991. Aspectos geológico-estruturais da sismicidade relacionada ao reservatório de Capivara (SP/PR). In: *II Congr. Int. Soc. Bras. Geofísica, Salvador, Proceedings,* **1,** 513–520.

Qiu, X., Priestley, K. & McKenzie, D., 1996. Average lithospheric structure of southern Africa, *Geophys. J. Int.,* **127,** 563–587.

Riccomini, C., Velázquez, V.F. & Gomes, C.B., 2004. Tectonic controls of the Mesozoic and Cenozoic alkaline magmatism in central-southeastern Brazilian Platform, in *Mesozoic to Cenozoic Alkaline Magmatism in the Brazilian Platform*, pp. 1–26, eds Comin-Chiaramonti, P. & Gomes, C.B., EDUSP-FAPESP, São Paulo, Brazil.

Rocha, M.P., 2003. Extension of upper mantle seismic tomography in SE and central Brazil using *P* waves, *MPhil thesis,* IAG, University of São Paulo, São Paulo (in Portuguese).

Schimmel, M., Assumpção, M. & VanDecar, J., 2003. Upper mantle seismic velocity structure beneath SE Brazil from *P*- and, S,-wave travel time inversions, *J. geophys. Res.,* **108**(B4), 2191, doi:10.1029/2001JB000187.

Seeber, L. & Armbruster, J.G., 1988. Seismicity along the Atlantic seaboard of the U.S.: intraplate neotectonics and earthquake hazard, in *The Geology of North America,The Atlantic Continental Margin: U.S.*, Vols 1–2, pp. 565–582, eds Sheridan, R.E. & Grow, J.A., Geol. Soc. Am.

Sleep, N.H., 2003. Fate of mantle plume material trapped within lithospheric catchment with reference to Brazil, *Geochem. Geophys. Geosyst.,* **4,** Art. No. 8509.

Sonder, L.J., 1990. Effects of density contrasts on the orientation of stresses in the lithosphere: relation to principal stress directions in the Tansverse Ranges, California, *Tectonics,* **9,** 761–771.

Stein, S., Cloetingh, S., Sleep, N.H. & Wortel, R., 1989. Passive margin earthquakes, stresses and rheology, in *Earthquakes at North-Atlantic Passive Margins: Neotectonics and Postglacial Rebound*, pp. 231–259, eds Gregersen, S. & Basham, P.W., Kluwer, Dordrecht.

Sykes, L., 1978. Intraplate seismicity, reactivation of pre-existing zones of weakness, alkaline magmatism, and other tectonism postdating continental fragmentation, *Rev. Geophys. Space Phys.,* **16,** 621–688.

Talwani, P., 1989. Characteristic features of intraplate earthquakes and the models proposed to explain them, in *Earthquakes at North-Atlantic Passive Margins: Neotectonics and Postglacial Rebound*, pp. 231–259, eds Gregersen, S. & Basham, P.W., Kluwer, Dordrecht.

Talwani, P. & Rajendram, K., 1991. Some seismological and geometric features of intraplate earthquakes, *Tectonophysics,* **186,** 19–41.

Thompson, R.N., Gibson, S.A., Mitchell, J.G., Dickin, A.P., Leonardos, O.H., Brod, J.A. & Greenwood, J.C., 1998. Migrating Cretaceous-Eocene magmatism in the Serra do Mar alkaline province, SE Brazil: melts from the deflected Trindade mantle plume, *J. Petrol.,* **39,** 1493–1526.

Tommasi, A. & Vauchez, A., 1997. Continental-scale rheological heterogeneities and complex intraplate tectono-metamorphic patterns: insights from a case-study and numerical models, *Tectonophysics,* **279,** 327–350.

VanDecar, J.C., James, D.E. & Assumpção, M., 1995. Seismic evidence for a fossil mantle plume beneath South America and implications for plate driving forces, *Nature,* **378,** 25–31.

Wilks, K.R. & Carter, N.L., 1990. Rheology of some continental lower crustal rocks, *Tectonophysics,* **182,** 57–77.

Yamabe, T.H. & Berrocal, J., 1991. A origem da atividade sísmica de Presidente Prudente (SP): induzida ou natural? In: *II Congr. Int. Soc. Bras. Geofísica, Salvador, Proceedings,* **1,** 521–528.

Yamabe, T.H. & Hamza, V.M., 1996. Geothermal investigations in an area of induced seismicity, northern São Paulo state, Brazil, *Tectonophysics,* **253,** 209–225.

Yang, Y. & Liu, M., 2002. Why North China is seismically active while South China remains largely aseismic? In: *AGU Fall Meeting, San Francisco, Abstracts, 2002*.

Zoback, M.L. & Richardson, R.M., 1996. Stress perturbation associated with the Amazonas and other ancient continental rifts, *J. geophys. Res.,* **101,** 5459–5475.